Available online at www.eccomasproceedia.org
Eccomas Proceedia COMPDYN (2023) 1499-1511

ECCOMAS
Proceedia

COMPDYN 2023
9th ECCOMAS Thematic Conference on
Computational Methods in Structural Dynamics and Earthquake Engineering
M. Papadrakakis, M. Fragiadakis (eds.)
Athens, Greece, 12-14 June 2023

DESIGN FOR ROBUSTNESS OF A PILOT BUILDING EQUIPPED WITH DISSIPATIVE FREE FROM DAMAGE STEEL CONNECTIONS

T. Golea[1], R. Tartaglia[2], M. Latour[3], M. D'Aniello[4], J.-F. Demonceau[1], R. Landolfo[4], and V. Piluso[3]

[1] University of Liège, Liège, Belgium
tudor.golea@uliege.be, jfdemonceau@uliege.be

[2] University of Sannio, Benevento, Italy
roberto.tartaglia@unina.it

[3] University of Salerno, Salerno, Italy
mlatour@unisa.it, v.piluso@unisa.it

[4] University of Naples, Naples, Italy
mdaniel@unina.it, landolfo@unina.it

Abstract

Recent research initiative aimed at reducing the structural damage and its inherent economic consequences in steel and steel-concrete composite structures after severe earthquakes led to the development of FREE from DAMage (FREEDAM) beam-to-column connections. The practical applicability and the benefits of using these connections for structures in seismic areas are currently demonstrated within an ongoing RFCS pilot project to be built on the campus of the University of Salerno. Amongst the different structural requirements, Eurocodes nowadays require providing the structures with an appropriate robustness when subjected to identified or unidentified accidental events by ensuring that the undergone damages are not disproportionate to the initiating cause. This paper presents the design for robustness of the pilot building. The results indicate that the loss of a column at the base floor induces the development of significant catenary action in the beams bridging over the lost column. The structural performance under the column loss scenario is primarily governed by the behaviour of beam-to-column joints subsequently identified as critical zones. The full-range behaviour of the FREEDAM joints was investigated through complex numerical simulations which allowed validating a simplified component-based spring model that can be adopted for the regular design of structures adopting this joint typology.

Keywords: Robustness, Colum loss, Dissipative joints, FREEDAM joints, Seismic devices, FE analysis.

ISSN:2623-3347
Peer-review under responsibility of the organizing committee of COMPDYN 2023.
doi: 10.7712/120123.10495.20893

1 INTRODUCTION

Experimental evidence [1] has shown that moment resisting frames (MRFs) with FREEDAM joints exhibit excellent seismic performances. The robustness of these structures in case of accidental events such as column loss scenarios, vehicle collisions, explosions, and fire has also been investigated [2]. Furthermore, EN 1990 [3] and EN 1991-1-7 [4] dealing with the design against accidental actions, expressly require ensuring appropriate robustness to any structure so that the risk of progressive collapse is mitigated and, most importantly, human losses are prevented in case of identifiable or unidentifiable accidental actions.

To ensure this robustness, the standard recommends different design approaches, the simplest amongst them being the so-called "tying method" which aims at ensuring an efficient horizontal/vertical tying system (continuity) between the structural members. However, previous studies [2,5] revealed that the robustness achieved through this method is questionable and frequently insufficient for accidental scenarios leading to the loss of a supporting column.

An alternative proposed in EN 1991-1-7 [3] is to consider the "notional removal of supporting elements", known as the alternative load path method, to verify if the structure exhibits sufficient robustness to survive the loss of a supporting member regardless of the triggering event. Therefore, this threat-independent method allows covering a wide range of foreseeable and unforeseeable accidental events and enables the designer to identify the potential key/critical structural members. Nonetheless, this approach requires advanced means of analysis incorporating geometrical and material nonlinearities. Within his paper, the application of this alternative method to a pilot building designed in the framework of the DREAMERS RFCS project and to be built on the Campus of the University of Salerno will be presented, demonstrating the added value coming from the use of FREEDAM connections exhibiting high rotation capacities.

2 CASE STUDY

2.1 General building layout

The DREAMERS pilot building was designed according to Eurocode 8 [6] and Italian design regulations [7]. The three-storey building has an approximate height of 12 m and plan dimensions of 25 m and 15 m on Y and X directions respectively (Figure 1). The structure is provided with lateral load-resisting systems made of MRFs located on its perimeter, whereas the inner bays consist of gravity frames. The COFRADAL260 steel-concrete composite slim floor system proposed by ArcelorMittal is adopted for all the floor slabs. This solution implies the partial encasement of floor beams into the slab. In this regard, the interior beams are made of cut-off HE300B and HE240B cross-sections (HEB300C and HEB240C in Figure 1). S355 steel grade is adopted for the structural elements with cross-sections consisting of HEB and IPE profiles. The loads considered in the structural design are reported in Table 1.

Load type	1^{st} floor	2^{nd} floor	3^{rd} floor
Dead load (kN/m^2)	5.35	5.35	4.15
Live load (kN/m^2)	3.0	3.0	-
Cladding (kN/m)	4.4	4.4	-
Snow load (kN/m^2)	-	-	0.6

Table 1: Design loads.

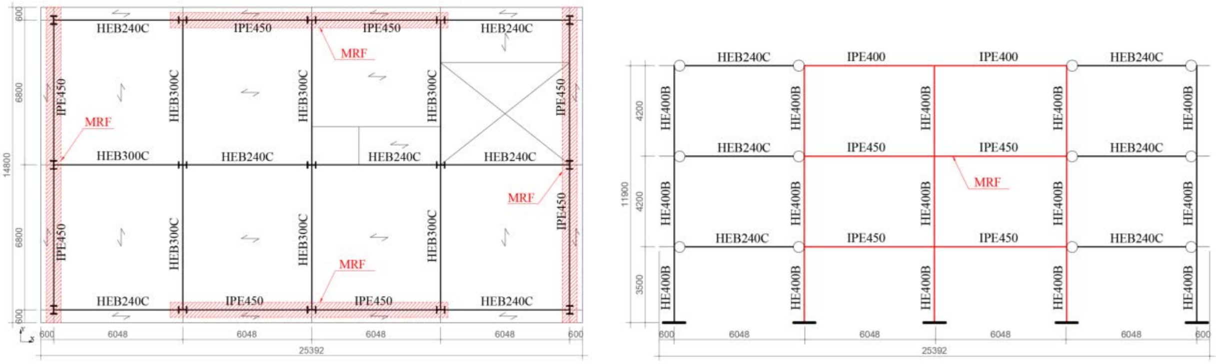

a) Plan view b) Elevation view

Figure 1: Plan view and elevation view of the pilot building

2.2 Specificities of beam-to-column FREEDAM joints

The perimeter MRFs of the pilot building are designed with dissipative zones concentrated in the beam-to-column joints with friction dampers (see Figure 2a). As demonstrated in a recent RFCS research project [8], these joints ensure high seismic performance in earthquake resistant structures due the wide and stable hysteretic response. Generally, the dissipative characteristics of these connections are tuned with respect to local (within the joint) and global (between the connected members) resistance hierarchy according to the Capacity Design principles. The seismic input energy is dissipated through friction in a damping device attached to the lower flange of the connected beam. The friction pads provided within the damper are made of steel plates coated with thermally sprayed material, and the whole damping device is fastened to the steel haunch by high-strength (HS) bolts with allowed sliding along the horizontal slotted holes provided on the L-stubs. The preload in the HS bolts is adjusted such that the sliding is initiated once the joint bending moment reaches the demand associated to the seismic or fundamental load combination at Ultimate Limit State (ULS).

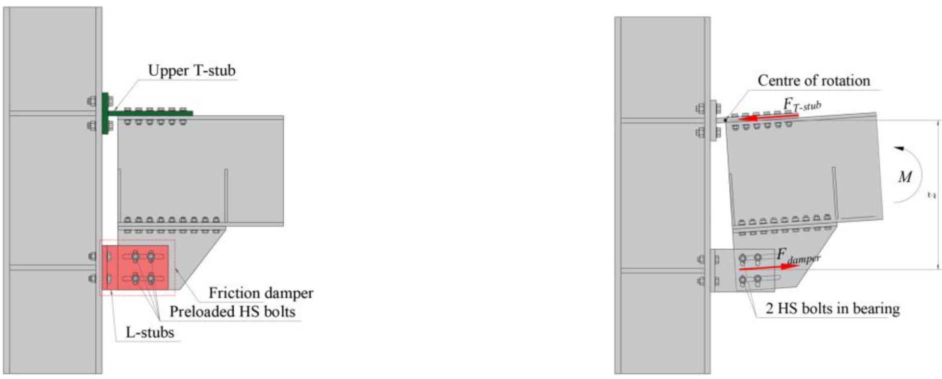

a) Joint general detailing b) Stroke-end limit condition under sagging

Figure 2: Particularities of FREEDAM joints.

Therefore, the sliding resistance of the joints is estimated such that it matches the bending moment demand associated to the ULS according to Eq. (1)

$$M_{j,Rd} = \mu_{d,k} n_s n_b \frac{F_{pd}}{\gamma_{creep}} z \tag{1}$$

where $\mu_{d,k}$ is the characteristic dynamic friction coefficient taken as 0.53, n_s is the number of friction surfaces, n_b is the number of preloaded bolts clamping the damper, F_{pd} is the design bolt preload, and z is the joint lever arm. The γ_{creep} safety factor accounts for the loss of the initial bolt preload due to relaxation (creep) phenomena and is taken equal to 1.15 [9].

Additional energy dissipation is envisaged through ductile plastic deformations in plate components (T-stub and L-stubs in Figure 2a) once the friction damper has reached its so-called "stroke-end" limit condition (Figure 2b). At this instance, the HS bolts clamping the damper are subjected to shear (2 HS bolts in bearing in Figure 2b), while other joint components (i.e., T-stubs, L-stubs, and plates) are submitted to bending, bearing, and tension/compression. The post-sliding behaviour of the FREEDAM joints is thus governed by the shear capacity of bolts and the ductile response of plate components. This range of behaviour is particularly of interest when considering the structural robustness. Indeed, in case of column loss scenario, the likelihood to reach the damper's sliding capacity is high due to the development of significant bending moments at the extremities of the beams above the lost column, associated to the apparition of significant rotations.

3 JOINT MODELLING

In daily design practice, the behaviour of joints is typically integrated in structural analyses through rotational springs simulating the response of joints under bending action. However, this modelling approach is not suitable when considering column loss scenarios. Indeed, under such scenarios, catenary actions develop in the beams above the lost column and so, the joints at the extremities of these beams are subjected to moment-axial force (M-N) interaction which cannot be modelled using a rotational spring. Within the present section, an alternative to accurately simulate the behaviour of FREEDAM joints subjected to M-N interaction is proposed (§ 3.1) and validated through comparisons to numerical simulation results from an advanced model built in Abaqus (§ 3.2 and § 3.3).

3.1 Simplified mechanical model for FREEDAM joints

Based on the component method recommended in EN 1993-1-8 [10], a simplified two-spring model for FREEDAM joints was developed and validated against experimental evidence by D'Antimo [11] and Santos et al. [12]. The model consists of two extensional springs (top and bottom) interconnected by rigid elements as represented in Figure 3a. A rigid shear spring ensures the transfer of shear forces at the beam ends.

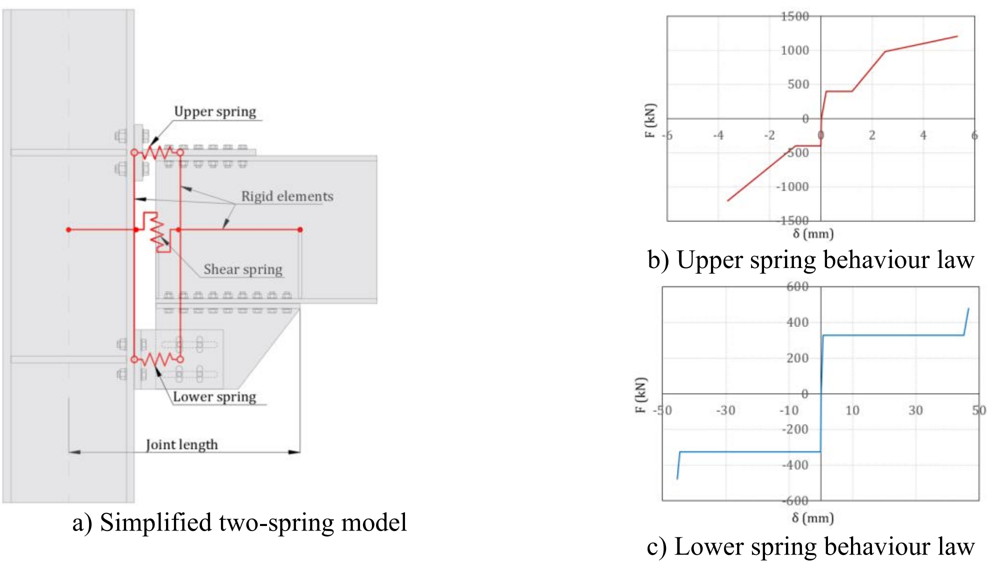

a) Simplified two-spring model

b) Upper spring behaviour law

c) Lower spring behaviour law

Figure 3: FREEDAM joint mechanical modelling.

The developed model accommodates the *M-N* interaction and accounts for the behaviour of basic joint components characterised by extensional springs with nonlinear behaviour laws (see Figure 3b-c) derived with the component method which has been adapted (i) to characterise both pre- and post-sliding behaviour of the FREEDAM joints and (ii) to predict the FREEDAM joint behaviour up to failure through the analytical computation of a strain-hardening stiffness and an ultimate strength according to [13].

3.2 Advanced finite element model

Numerical simulations using implicit dynamic analyses were performed using the ABAQUS 2017 software [14]. The FE model (see Figure 4) consisted of eight-node brick element with reduced integration (C3D8R). The mesh density was defined based on sensitivity analyses already performed in previous studies [15].

True stress-true strain curves derived from coupon tensile testing were adopted for all of the materials. Steel S355 was used for all the elements while, for the bolts, 10.9 grade was adopted. Threads in the bolts were not directly modelled, since the bolts are modelled as combination of three cylindrical parts, with the shank having the nominal diameter of the bolt as depicted in Figure 4b. Von Mises yield criterion with combined isotropic and combined hardening was used throughout the analyses.

Contact between parts was modelled as surface-to-surface interaction with penalty friction formulation. Steel-to-steel contact was characterised through a friction coefficient of 0.3, and a dynamic (mean) friction coefficient equal to 0.59 was used for the friction shims as adopted in [15].

Loads were applied as quasi-static taking into account the geometrical non-linearities, while the bolt preload is applied by means of bolt load option available in Abaqus.

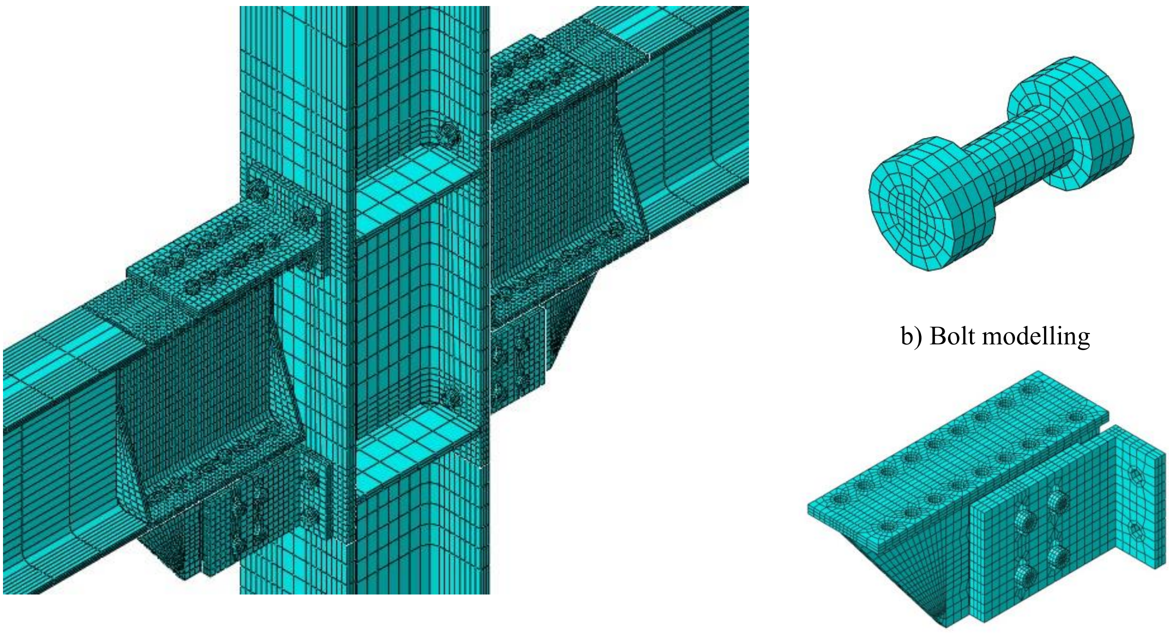

a) General 3D view

b) Bolt modelling

c) Friction damper modelling

Figure 4: Advanced FE model of the FREEDAM joint.

3.3 Validation of the simplified two-spring model

To validate the simplified two-spring model, a double-sided joint was extracted from the perimeter frame of the pilot building and analysed in isolation as shown in Figure 5. Two loading cases were considered: i) monotonic loading (Figure 5b) with bending moments (sagging and hogging) applied up to the failure of the joint and ii) column loss scenario with axially restrained beams as shown in Figure 5c. The two-spring model was implemented in the homemade finite element software Finelg [16] which allows performing different types of analyses (e.g., elastic, nonlinear, static/dynamic) with account for geometric and material non-linearities.

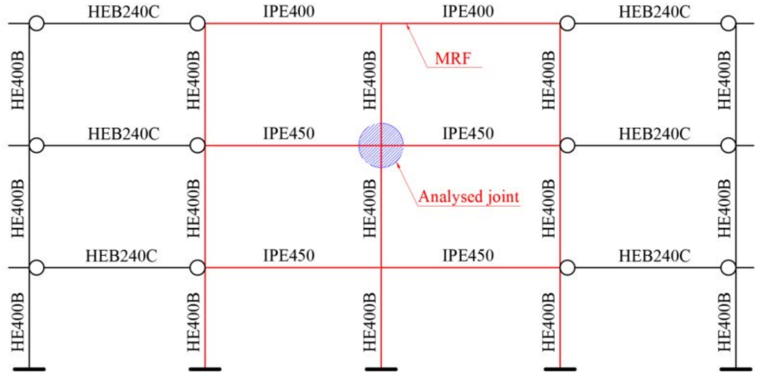

a) Joint location

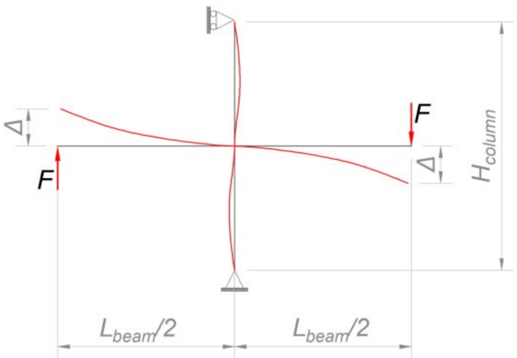

b) Monotonic loading

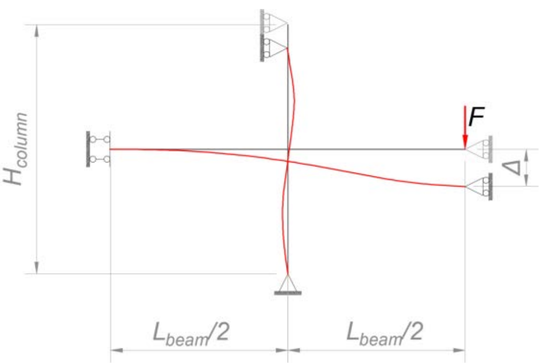

c) Column loss scenario

Figure 5: Analysed FREEDAM joint.

The results reported in Figure 6 show that the simplified spring model accurately predicts the initial stiffness of the joints as well as the onset of the sliding within the friction damper and the attainment of the stroke end phase. However, although the joint's stiffness in the post-slippage phase is predicted with reasonable accuracy, the ultimate moment resistance and the ultimate rotation capacity are significantly lower than the ones provided by the advanced FE models. This difference is mainly due to the fact that the two-spring model is based on the component method which, as recommended in EN 1993-1-8 [10], only allows for the prediction of the plastic resistance of the joints and of their components. Jaspart et al [13] extended the component method to predict the ultimate resistance and the associated deformation capacity using safe assumptions. In the advanced FE models, it is possible to go beyond the ultimate stress and strain of the material considering true stress-truss strain behaviour laws. However, the observed difference between the simplified and the advanced models appears to be important and questionable. This issue will be investigated through experimental tests performed at the University of Liege in the near future.

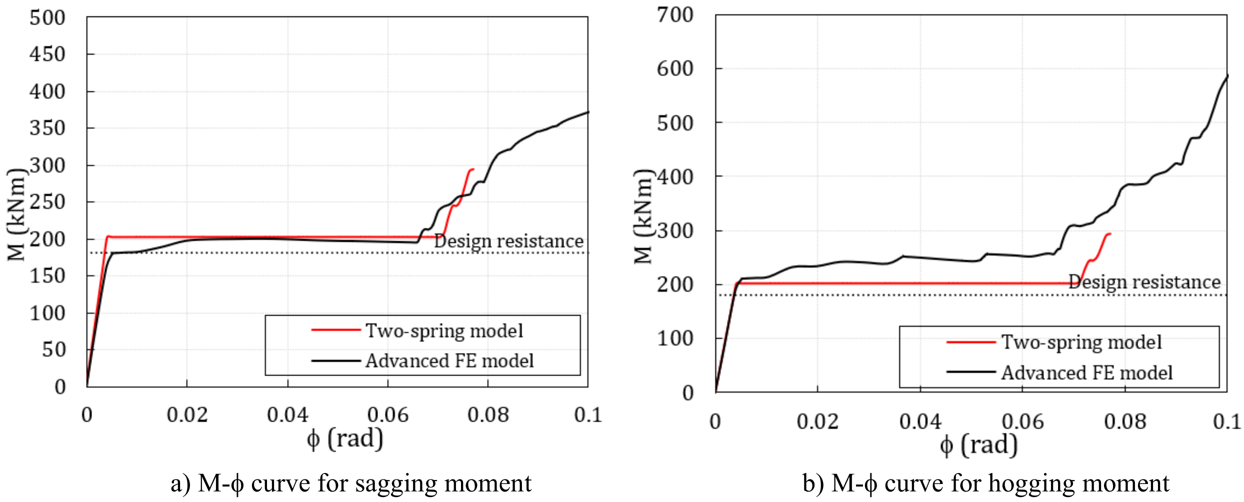

Figure 6: Simplified model validation – Monotonic loading.

As shown in Figure 7, for the second load case (column loss scenario in Figure 5c), the two models converge in terms of initial stiffness and evolution of internal forces in the modelled substructures. The predictions for the ultimate resistance and rotation capacities are in reasonable agreement considering that no material softening is considered in the simplified two-spring model.

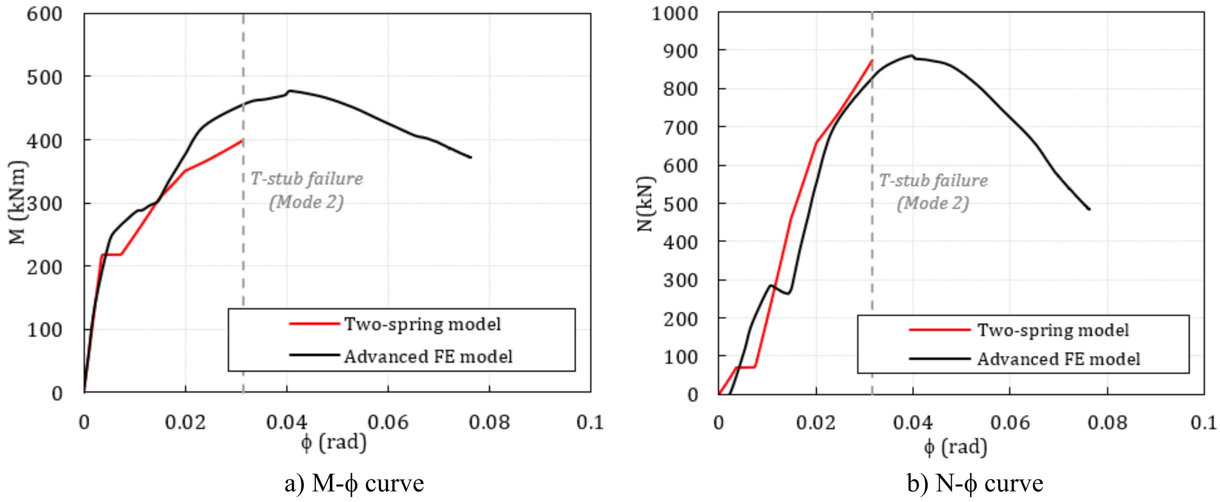

Figure 7: Simplified model validation – Column loss scenario.

Given the development of catenary action in the beam connected to the lost column (Figure 7b), the failure mode of the joint changes from the shear failure of the damper bolts under pure bending (first analysed case) to the failure of the upper T-stub in bending. The predicted failure modes are similar in both models, thus representing an additional validation criterion.

The obtained results allow adopting the simplified two-spring model for global structural analyses, as performed hereafter, knowing that this model could be on the safe side for the prediction of the ultimate joint resistance.

4 ROBUSTNESS ASSESSMENT UNDER COLUMN LOSS SCENARIO

4.1 Structural model

The column loss was numerically simulated through nonlinear static analyses using Finelg software [16]. The structural model was built using classical 3D beam elements with material behaviour laws incorporating the yielding plateau and the strain hardening of steel material. The provisions of prEN 1993-1-14 [17] were used to define the nonlinear behaviour law for the S355 steel as illustrated in Figure 8.

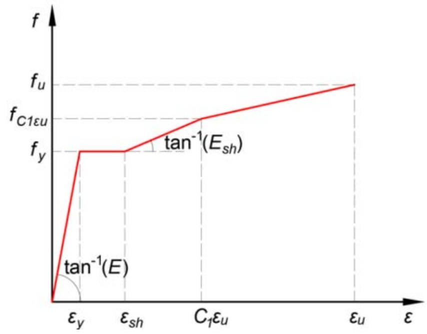

Figure 8: Material constitutive law.

The composite slab was not explicitly modelled; however, given its important contribution to the structural response under lateral loads through the diaphragm effect, the latter was considered through a horizontal bracing system at the level of each floor as illustrated in Figure 9 (highlighted in red) and as recommended in [5]. Rigid beam elements with circular cross-section were used to model these bracing elements such that the relative horizontal displacements between the columns at the level of each slab are prevented, thus simulating the rigid diaphragm provided by the slabs. It is worth noting that this modelling choice covers only partially the behaviour of the slab. However, limited data is available on the post-limit behaviour of the COFRADAL260 slim floor solution, and the modelling used herein may be seen as conservative since the contribution of the slab in terms of plastic mechanism and membrane actions are neglected.

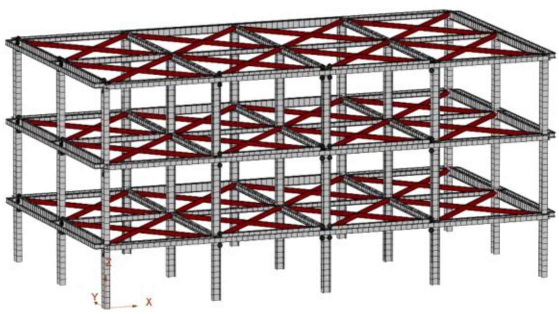

a) 3D view

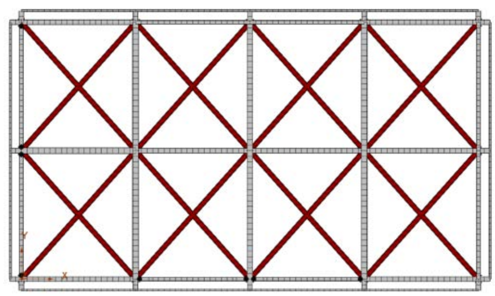

b) Slab diaphragm effect

Figure 9: Structural model.

The gravity loads were applied to the supporting beams as uniform line loads estimated based on the direction of slab load transfer and tributary areas. The accidental load combination was considered in the analyses according to the prescriptions of EN 1990 [3].

The loss of a supporting column in the perimeter MRF was simulated through a two-sequence analysis. At first, the lost column was replaced by a reaction force equal to the column design axial force N_d in the accidental load combination. The second sequence initiates a nonlinear analysis in which an incremental downward force $F=\lambda N_d$ is applied at the same location as N_d as depicted in Figure 10.

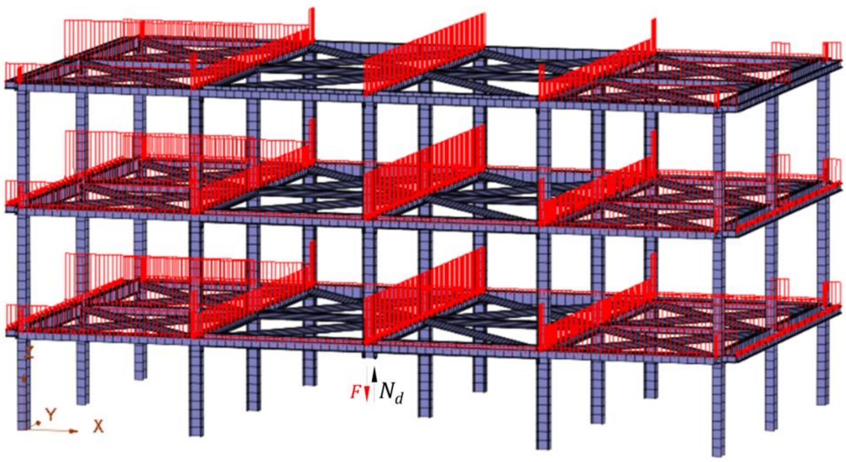

Figure 10: Perimeter column loss loading sequence.

The evolution of the applied incremental force F plotted against the vertical displacement of the force application point characterises the full nonlinear structural response under the column loss. The so-obtained force-displacement F-d (pushdown) curve is used to assess the structural robustness.

4.2 Results and discussion

Figure 11 depicts the structural behaviour of the pilot building under the assumed perimeter column loss. An additional validation criterion is given by the predicted "pseudo-plastic" mechanism developed in the analysed frame once all the FREEDAM joints reach their friction resistance. The analytical prediction for the vertical force required to reach this mechanism (P_{pr}) is in good agreement with the numerical results (see the match between P_{pr} and the plateau in Figure 11b).

The large rotational capacity of the dissipative joints provided in these two bays allows for the development of significant membrane forces in the beams (880 kN) above the lost column. This enables the structure to withstand the column loss with significant residual strength (F_u=1.76Nd) and a Demand/Capacity ratio D/C=0.57.

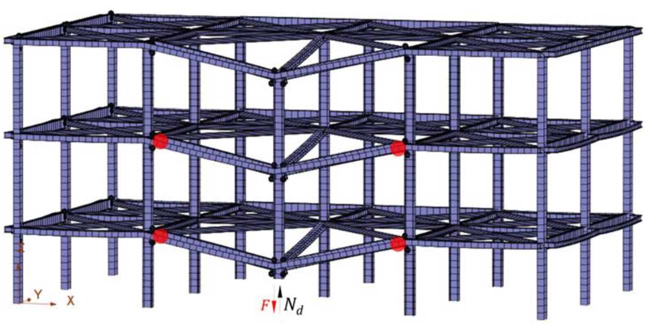

a) Deformed shape

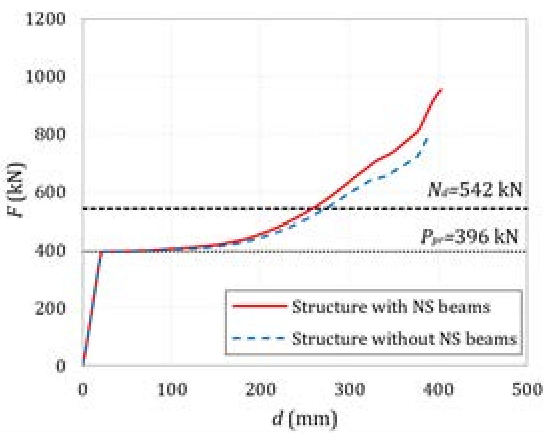

b) Force-displacement curve

Figure 11: Structural response under the column loss.

The structural model incorporates some of the non-structural (NS) members such as the UPN beams supporting the façade. These beams are located on the perimeter of the structure and could contribute to the overall robustness of the frame. This is demonstrated in Figure 11b through comparisons between the response of the structure with and without the NS beams. The results reveal that the tensile forces in these non-structural beams reach values of 330 kN. Obviously, if the end-connections are not capable of transferring these tensile forces, the contribution of the NS beams to the structural robustness should be neglected. Even so, the structure proves to be robust enough to withstand the column loss with a D/C=0.68.

The collapse is triggered by the successive failure of the FREEDAM joints located at the first two storeys (highlighted in red in Figure 11a). In Section 3.3, it has been shown that these joints subjected to hogging moment and axial load fail as soon as the ultimate resistance of the T-stub in bending component is reached. The simulation performed on the full structural model confirms this expectation.

Figure 12 shows the variation of internal forces with respect to the chord rotation in the failing joints. A qualitative comparison is made between the response of the joint sub-assembly in Section 3.3 and as part of the global structural model. The overall response is similar, yet some discrepancies in terms of deformability and rotation are observed. These may be ascribed to the boundary conditions imposed in the model simulating the joint in isolation (i.e., fully axially restrained beams).

The evolution of internal forces depicted in Figure 12 reveals some important peculiarities related to the behaviour of the FREEDAM joints and the fact that the structural response of building equipped with such joints is quite different when compared to structures with conventional joints subjected to column losses.

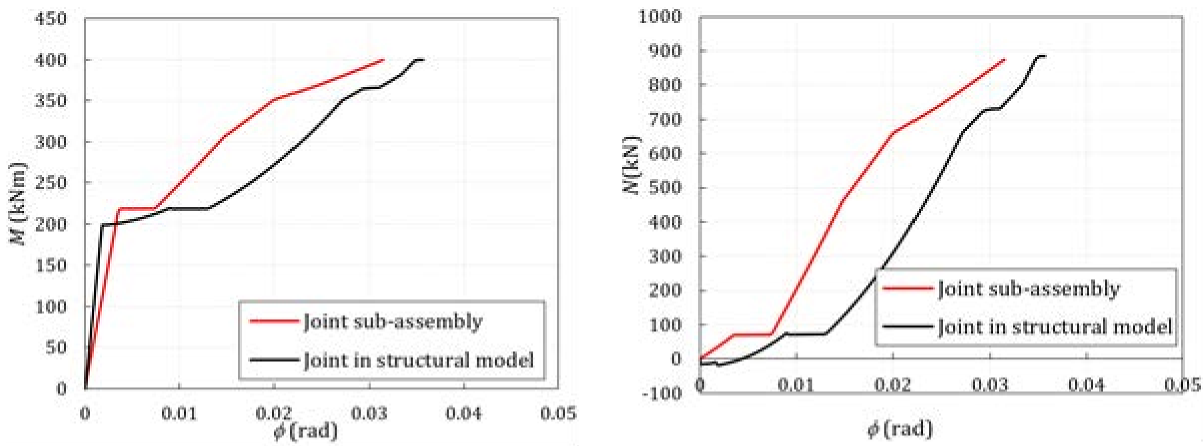

a) Moment-chord rotation curve b) Axial force-chord rotation curve

Figure 12: Internal forces in the FEEEDAM joints.

More specifically, the bending moment acting on the joint increases even after membrane forces start developing in the beams connected to the lost column. This can be seen as in opposition to what is normally observed in structures with conventional semi-rigid joints as proved in [18]–[20] among others.

This difference is related to the influence of the friction damper response on the distribution of internal forces within the joint. The evolution of forces in the two-springs of the simplified model depicted in Figure 13 may clarify this issue. Once the damper has reached its friction resistance, the overall joint has reached its sliding moment capacity and rotates with virtually no further moment increase. As soon as the vertical displacements become significant (approx. 170 mm and 0.015 rad chord rotation), the beams are engaged in catenary action and significant axial tension develops. This tension is eccentrically transferred from the beam cross-section to the joint cross-section, thus inducing a bending moment. Furthermore, since the damper (lower spring) enters in the slippage phase, its resistance remains constant (friction resistance). To ensure the compatibility of displacements and the equilibrium on the joint cross section, the upper spring (T-stub) is overloaded in tension, which leads to the increase of the bending moment appearing at the joint level and to the subsequent failure of the T-stub (upper spring).

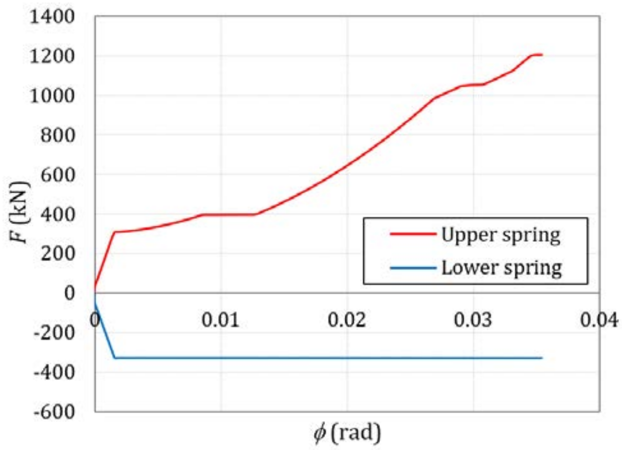

Figure 13: Evolution of forces in the springs of the simplified model for FREEDAM joints.

5 CONCLUSIONS

The investigations presented in this paper allow concluding that the pilot building proves to be sufficiently robust to survive to the loss of a perimeter column located in the moment resisting frame equipped with FREEDAM joints. Even if the potential contribution of the secondary beams that support the façade are neglected, the structure exhibits a significant overstrength to withstand this accidental scenario.

Particularities related to the behaviour of the FREEDAM joints were highlighted. These concern the evolution of internal forces at the joint level which is rather different than the one observed in structures with traditional semi-rigid joints. The increase of the bending moment in the joints along with the increase of the tensile action in the beams connected to the lost column is caused by the long slippage phase in the damping device and internal redistribution of forces within the joints.

Advanced FE analyses performed on the dissipative joints allowed validating a simplified two-spring model that accommodates the moment-axial force interaction at the joint level and can be effectively used in global structural analyses for regular design or research-oriented investigations. However, specific aspects related to the ultimate capacities of joint components and the accuracy of component characterisation through the component method are still to be addressed. In particular, the simplified mechanical model seems to be overconservative in terms of ultimate moment resistance. This will be further investigated through experimental tests on the joints to be performed at the University of Liege.

ACKNOWLEDGEMENTS

The work presented in this paper was carried out within the DREAMERS research project (GA n°: 101034015). Financial support from the Research Fund for Coal and Steel is gratefully acknowledged.

REFERENCES

[1] FREEDAM PROJECT. http://www.freedamproject.eu/.

[2] T. Golea, A. F. Santos, J.-P. Jaspart, M. Latour, A. Santiago, and J. Demonceau, Design for robustness of steel structures with dissipative FREEDAM joints, *International Journal of Earthquake Engineering*, vol. 2, 2022.

[3] EN 1990, *Eurocode 0 - Basis of structural design*, Brussels: European Committee for Standardisation, 2002.

[4] EN 1991-1-7, *Eurocode 1 - Actions on structures - Part 1-7: General actions - Accidental actions*, Brussels: European Committee for Standardisation, 2006.

[5] J.-F. Demonceau, T. Golea, J.-P. Jaspart, A. Elghazouli, Z. Khalil, A. Santiago, A.F. Santos, L.S. da Silva, U. Kuhlmann, G. Skarmoutsos, N. Baldassino, R. Zandonini, M. Bernardi, M. Zordan, F. Dinu, I.M. Marginean, D. Jakab, D. Dubina, F. Wertz, K. Weynand, R. Obiala, M. Candeias, M. Charlier, and O. Anwaar, *Design recommendations against progressive collapse in steel and steel-concrete buildings (FAILNOMORE)*, ECCS – European Convention for Constructional Steelwork, 2021

[6] EN 1998-1, *Eurocode 8 - Design of structures for earthquake resistance - Part 1: General Rules, seismic actions and rules for buildings*, European Committee for Standardisation, 2004.

[7] NTC, *Norme techniche per le construzioni." Ministero delle Infrastrutture e dei Trasporti,* 2018.

[8] FREEDAM (2015-2018): *FREE from DAMage Steel Connections*, Fund for Coal and Steel Grant Agreement No. RFSR-CT-2015-00022.

[9] G. F. Cavallaro, M. Latour, A. B. Francavilla, V. Piluso, and G. Rizzano, Standardised friction damper bolt assemblies time-related relaxation and installed tension variability, *Journal of Constructional Steel Research*, no. 141, pp. 145–155, 2018.

[10] EN 1993-1-8*, Eurocode 3 - Design of steel structures - Part 1-8: Design of joints*, Brussels: European Committee for Standardisation, 2005.

[11] M. D'Antimo, *Impact characterization of innovative seismically designed connections for robustness application*, PhD Thesis, Université of Liège, 2020.

[12] A. F. Santos, A. Santiago, M. Latour, and G. Rizzano, Analytical assessment of the friction dampers behaviour under different loading rates, *Journal of Constructional Steel Research*, vol. 158, pp. 443–459, 2019.

[13] J.-P. Jaspart, A. Corman, and J.-F. Demonceau, *Ductility assessment of structural steel and composite joints*, 2019.

[14] Dassault Systèmes, *ABAQUS*, 2017.

[15] R. Tartaglia, M. D'Aniello, A. Campiche, and M. Latour, Symmetric friction dampers in beam-to-column joints for low-damage steel MRFs, *Journal of Constructional Steel Research*, vol. 184, 2021.

[16] FineLg, *Nonlinear finite element analysis program*, 2019.

[17] prEN 1993-1-14, *Design of steel structures - Part 1-14: Design assisted by finite element analysis*, European Committee for Standardisation, Brussels, 2021.

[18] J.-F. Demonceau, *Steel and composite building frames: sway response under conventional loading and development of membrane effects in beams further to an exceptional action*, PhD Thesis, Université de Liège, 2008.

[19] I.M. Marginean, *Robustness of moment steel frames under column loss scenarios*, PhD Thesis, Politehnica University of Timisoara, 2017.

[20] A. Kozlowski and D. Kukla, Experimental Tests of Steel Unstiffened Double Side Joints with Flush and Extended End Plate, *Archives of Civil Engineering*, vol. 65, no. 4, pp. 127–154, 2019.